JOTCS B
Journal of the Turkish Chemical Society
Section: B
Chemical Engineering
TURKISH CHEMICAL SOCIETY

Characterization of SiO_2 Thin Films Deposited by LPCVD

Fatma Betul Akgul Taner *

TUBITAK-BILGEM, Kocaeli, Turkiye

Abstract: In this study, SiO_2 film grown at different pressures using TEOS (tetraethyl orthosilicate) and O_2 gas was characterized by LPCVD (Low Pressure Chemical Vapor Deposition) method. The effect of high temperature annealing processes on the SiO_2 film structure was investigated. SiO_2 growth rate, etch rate, refractive index, stress, curvature values, film densities, and film structures were investigated with different analysis methods. In addition, impurities arising from the by-products of the reaction of TEOS and O_2 were detected in the SiO_2 film. AFM and RAMAN were used for the contamination detection analysis.

Keywords: LPCVD, SiO_2, film characterization.

Submitted: December 31, 2024. **Accepted:** August 19, 2025.

Cite this: Akgul Taner, F. B. (2025). Characterization of SiO2 Thin Films Deposited by LPCVD. *Journal of the Turkish Chemical Society Section B: Chemical Engineering*, *8*(2), 213–222. https://doi.org/10.58692/jotcsb.1607616

***Corresponding author. E-mail:** betul.taner@tubitak.gov.tr.

1. INTRODUCTION

The continuous advancement of semiconductor technologies has highlighted the critical importance of precise and reliable thin-film deposition techniques, particularly for silicon dioxide (SiO_2), which serves as a fundamental material in a wide range of applications, including hard masks and dielectric layers (Holzer et al., 2007). Among the available deposition methods, Plasma-Enhanced Chemical Vapor Deposition (PECVD), Atmospheric Pressure CVD (APCVD), and Low-Pressure CVD (LPCVD) are widely employed for fabricating SiO_2 films on silicon substrates (Rajib et al., 2016).

LPCVD, in particular, offers distinct advantages over other techniques due to its process stability, excellent film uniformity, and reduced contamination. The method involves the use of horizontal or vertical furnaces operating under low-pressure conditions to ensure uniform film growth on heated substrates. Notably, the absence of carrier gases in LPCVD systems minimizes particle generation and enhances surface homogeneity (Seshan, 2002).

Tetraethyl orthosilicate (TEOS) is commonly used as a silicon precursor in LPCVD processes due to its thermal stability and suitability for low-temperature deposition. TEOS-based SiO_2 films are known for their superior step coverage, low residual stress, and favorable mechanical and optical properties (Vamvakas et al., 1998).

In this study, SiO_2 thin films were deposited via LPCVD using TEOS and oxygen under controlled low-temperature conditions. Various characterization techniques were employed to evaluate the deposition rate, etch rates (wet and dry), FTIR spectra, roughness, density, residual stress, refractive index, and AFM surface morphology of the SiO_2 films. These analyses were conducted for both as-deposited and thermally annealed films to investigate the influence of post-deposition treatment on the film properties.

2. MATERIALS AND METHOD

2.1. Deposition by LPCVD

Silicon dioxide films were deposited using the Tempress LPCVD furnace system, the configuration of which is illustrated in Figure 1. The experiments were conducted on 6-inch p-type silicon wafers, 625 µm thick, with a [100] crystal orientation. Prior to deposition, the wafers underwent standard RCA cleaning followed by immersion in diluted HF. The

horizontal furnace, depicted in Figure 1, was electrically heated via resistance elements and housed a quartz boat with a capacity of 50 wafers, which were vertically positioned in individual slots (Sharma et al., 2014). Additionally, the temperature profile of the SiO_2 deposition process is shown in Figure 2. Deposition was performed at 700 °C, with gas flows of 75 sccm O_2 and 25 sccm TEOS. The process pressure ranged from 200 to 600 mT.

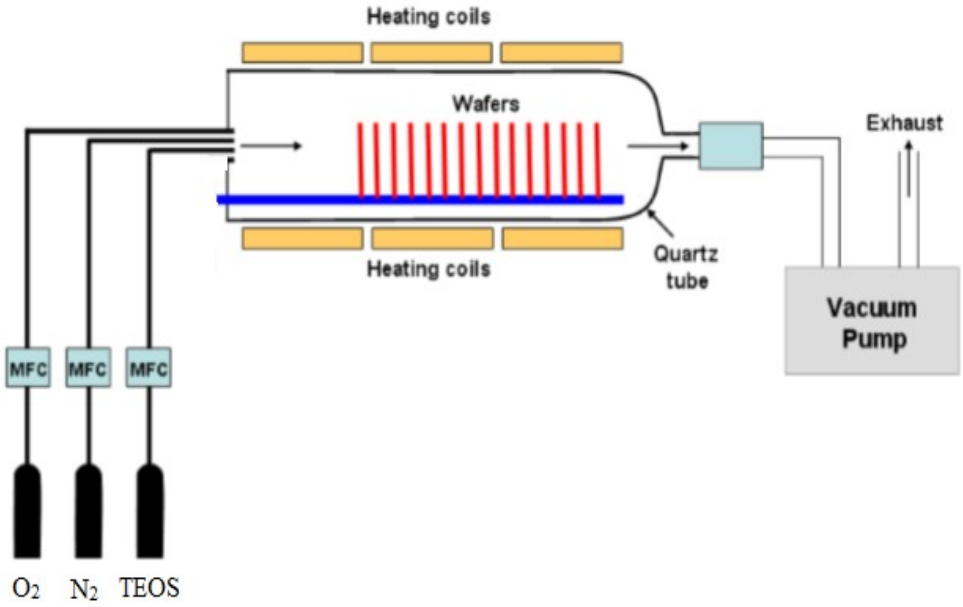


Figure 1: Schematic of LPCVD furnace system.

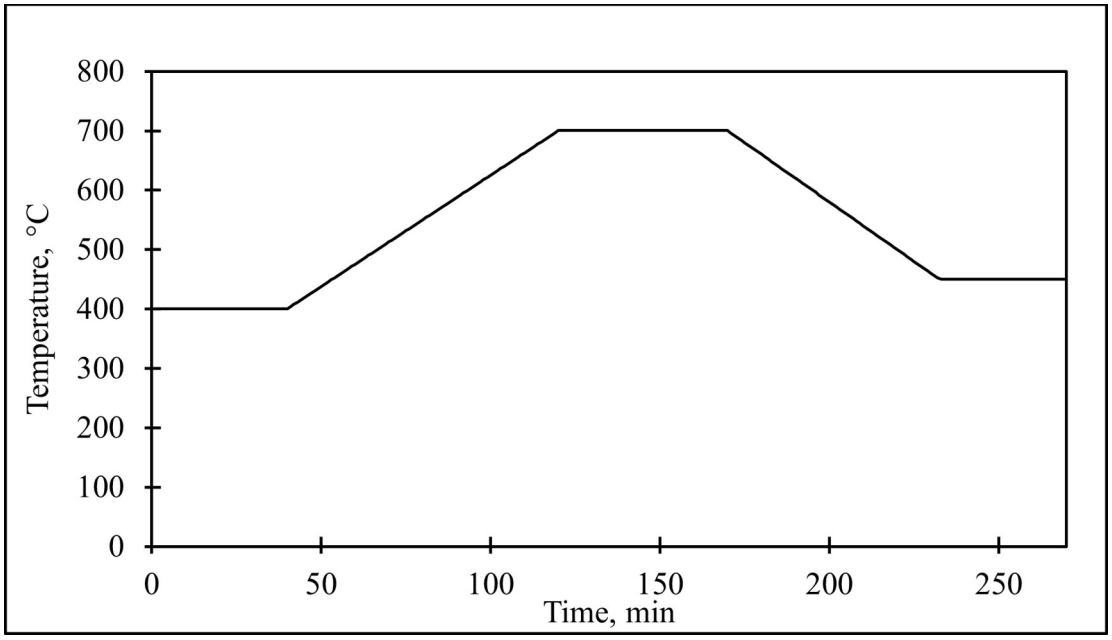


Figure 2: Temperature profile of the LPCVD furnace during SiO_2 film deposition.

2.1. Annealing processes

The SiO_2 films deposited in the LPCVD furnace were subsequently annealed in a Tempress diffusion furnace. The annealing process was carried out at a temperature of 1000 °C for a duration of 60 minutes, with a nitrogen gas flow rate of 4 standard liters per minute (slm).

2.2. Deposition rate

Film thickness was measured using Nanometrics equipment. The deposition rate was determined by dividing the film thickness by the deposition time, and it was expressed in units of angstroms per minute (Å/min).

2.3. Dry etching

Dry etching processes were performed in the RIE (Reactive Ion Etching) reactor. The platen generator power was set to 150 W, while the pressure inside the reactor was maintained at 80 mT. The flow rates of the feed gases were as follows: 35 sccm (standard cubic centimeters per minute) for CHF_3, 15 sccm for CF_4, and 1 sccm for O_2.

2.4. Wet etching

Wet etching processes were carried out using a 1:10 mixture of Buffered Oxide Etchant (BOE) solution at room temperature.

2.5. FTIR analyses

The chemical structures of the deposited SiO_2 films were examined using Fourier Transform Infrared Spectroscopy (FTIR) in the wavenumber range of 400 to 4000. Prior to measurement, the samples were held within the holder for 5 minutes to eliminate unwanted substances that may have been adsorbed on the film, such as H2O and CO2.

2.6. Refractive Index

The refractive index of the SiO_2 films was measured using J.A. Woollam Co. Ellipsometry. The measurements were conducted at a wavelength of 632.28 nm, with a spot size of approximately 1 nm and an incidence angle of 70º. To ensure accuracy, the equipment performed the measurement by taking readings at the same location 10 times and then calculating the average value.

2.7. Residual stress

The stress measurement was performed using a profiler system. The system employed a laser array to map the three-dimensional curvature and stress of semiconductor wafers. The scanning resolution achieved by the laser array was 2 µm. In the LPCVD system, thin films were deposited on both sides of the silicon wafer.

In order to assess the influence of the deposition process on stress, it was necessary to perform backside etching of the films. The initial curvature of the uncoated wafer was used as a baseline. Post-deposition, the alteration in curvature was then translated into the average residual stress within the film using Stoney's equation. After the deposition process, the change in curvature was converted to the average residual stress in the film using Stoney's equation. This allowed for the evaluation of the stress induced by the deposition of the thin films

The Stoney formula is widely used (Zhu et al., 2017).

$$\sigma_f t_f = \frac{E_s h^2}{6(1-\nu)R}$$

where σf is the residual stress causing deflection; ν is the Poisson’s ratio of the silicon wafer; Es is the elastic modulus of the silicon wafer; tf and h are the damage layer and silicon wafer thicknesses, respectively, and R is the deflection radius of curvature (Zhu et al., 2017).

2.8. Film density

The density of the SiO_2 film was determined using the following procedure: Initially, the mass of the wafers with LPCVD oxide film was measured. Subsequently, after the removal of the backside oxide, another mass measurement was conducted. The difference in mass corresponds to the mass of the SiO_2 film present on a single surface of the wafer.

To calculate the SiO_2 film density (in g/cm3), the ratio of the mass of the SiO_2 film to the surface volume of the wafer was determined (Zanotti et al., 1993).

2.9. Determination of contamination

To assess the contamination present at the Si/SiO_2 interface and within the volume of the films, Atomic Force Microscopy (AFM) and Raman spectroscopy techniques were employed (Viana et al., 2001).

AFM was used to examine the surface morphology and topography of the samples at the nanoscale. It provided valuable information regarding the presence of any surface defects, roughness, or contamination on the Si/SiO_2 interface.

Raman spectroscopy, on the other hand, was utilized to analyze the vibrational modes of the SiO_2 films. It helped identify the structural characteristics of the films and detect any potential impurities or deviations from the desired SiO_2 composition.

By combining the results from AFM and Raman spectroscopy, a comprehensive evaluation of both the interface contamination and the film quality in terms of structure and composition could be achieved.

3. DISCUSSION

3.1. Deposition rate

Table 1 presents the deposition rates of silicon dioxide films grown at different pressures. As expected, the deposition rate increased with increasing pressure, consistent with findings reported in the literature (Sharma et al., 2014; Viana et al., 2001).

After annealing the SiO_2 films deposited at varying pressures, it was observed that the film deposited at 200 mT exhibited a greater reduction in thickness, whereas the film deposited at 600 mT showed a smaller decrease.

Such a reduction in thickness during annealing is a common phenomenon in oxide films. In the case of LPCVD-deposited films, the observed shrinkage in TEOS-based SiO_2 indicates a porous film structure. Therefore, the results in Table 1 suggest that lower deposition pressures correspond to higher porosity in the SiO_2 films (Ritala et al., 2011).

Table 1: Deposition rates and thickness variations of SiO_2 films.

Pressure (mT)	Deposition Rate (Å/min)	Variation of thickness (%)
200	52.85±4	-6.29±0.3
300	82.75±5	-4.87±0.3
600	90.56±5	-3.99±0.3

3.2. Etching rates

Table 2 presents the dry etching rates of annealed and non-annealed LPCVD SiO_2 films grown at different pressures. It can be observed that the deposition pressure had no significant impact on the etching rates. However, annealing caused a slight reduction in the etching rate. This decrease can be attributed to the heat treatment reducing the film's porosity, thereby enhancing its resistance to etching (Ritala et al., 2011). Notably, the effect of annealing was consistent across all three deposition pressures.

Table 2: Dry etching rates of SiO_2 films.

Pressure (mT)	Sample	Etching rates (Å/min)
200	Non-annealed	1276±25
	Annealed	1176±14
300	Non-annealed	1200±17
	Annealed	1173±13
600	Non-annealed	1240±24
	Annealed	1171±12

Table 3 presents the wet etching rates of annealed and non-annealed LPCVD silicon dioxide films deposited at different pressures. Annealing had a pronounced effect on the etching rate, leading to a noticeable decrease across all etching solutions. Similar to the dry etching results, the deposition pressure had no significant influence on the wet etching rate. As expected, increasing the concentration of the HF solution resulted in a substantial increase in the etching rate of the SiO_2 films.

Table 3: Wet etching rates of SiO_2 films.

Pressure (mT)	Sample	Etching Rates (Å/min)		
		1:100 HF	1:7 Ultraetch (16.5 °C)	1:10 BOE
200	Non-annealed	174±20	3059±42	2142±22
	Annealed	40±4	1178±32	976±24
300	Non-annealed	153±18	2845±35	2264±30
	Annealed	36±4	1113±24	906±18
600	Non-annealed	164±20	2983±35	2222±21
	Annealed	37±4	1088±21	952±13

3.2. FTIR analyses

Fourier Transform Infrared (FTIR) spectroscopy was employed to analyze the chemical composition of the films, with the characteristic peak positions summarized in Table 4 (Ritala et al., 2011). The corresponding FTIR spectrum is shown in Figure 3, clearly displaying the absorption bands associated with Si-O-Si bonds. Specifically, the spectrum reveals peaks corresponding to Si-O-Si stretching, bending, and rocking vibrations at approximately 1070-1090 cm^{-1}, 810-820 cm^{-1}, and 460 cm^{-1}, respectively.

Table 4: FTIR peak values of SiO_2 films.

Pressure (mT)	Sample	Wavenumber (cm^{-1})		
		Si-O-Si streching	Si-O-Si bending	Si-O rocking
200	Non-annealed	1072	818	450
	Annealed	1089	813	460
300	Non-annealed	1074	816	450
	Annealed	1089	813	456
600	Non-annealed	1072	818	450
	Annealed	1086	814	456

After annealing the SiO_2 films, shifts in the peak positions corresponding to Si-O-Si bonds were observed across the entire film thickness (McCann et al., 2001). Notably, no discernible peaks associated with hydroxyl groups (3200–3600 cm-1) were detected (McCann et al., 2001). The absence of these peaks is attributed to the 90-minute post-deposition cool-down step, which likely acts similarly to a nitrogen annealing process by promoting the removal of water molecules from the film, thereby enhancing its chemical stability (Zhi et al., 2024; Gerelt-Od et al., 2024). This phenomenon reduces the film's moisture sensitivity by eliminating excess oxygen, resulting in a silicon-rich composition with improved chemical robustness. Such structural and compositional changes contribute positively to both the overall film quality and its electrical properties (Li et al., 2024). The shift in FTIR peak positions induced by annealing, along with the elimination of hydroxyl groups, reflects thermally driven improvements in the film's structure and chemistry. These enhancements may positively impact the performance of the film in integrated circuit fabrication processes.

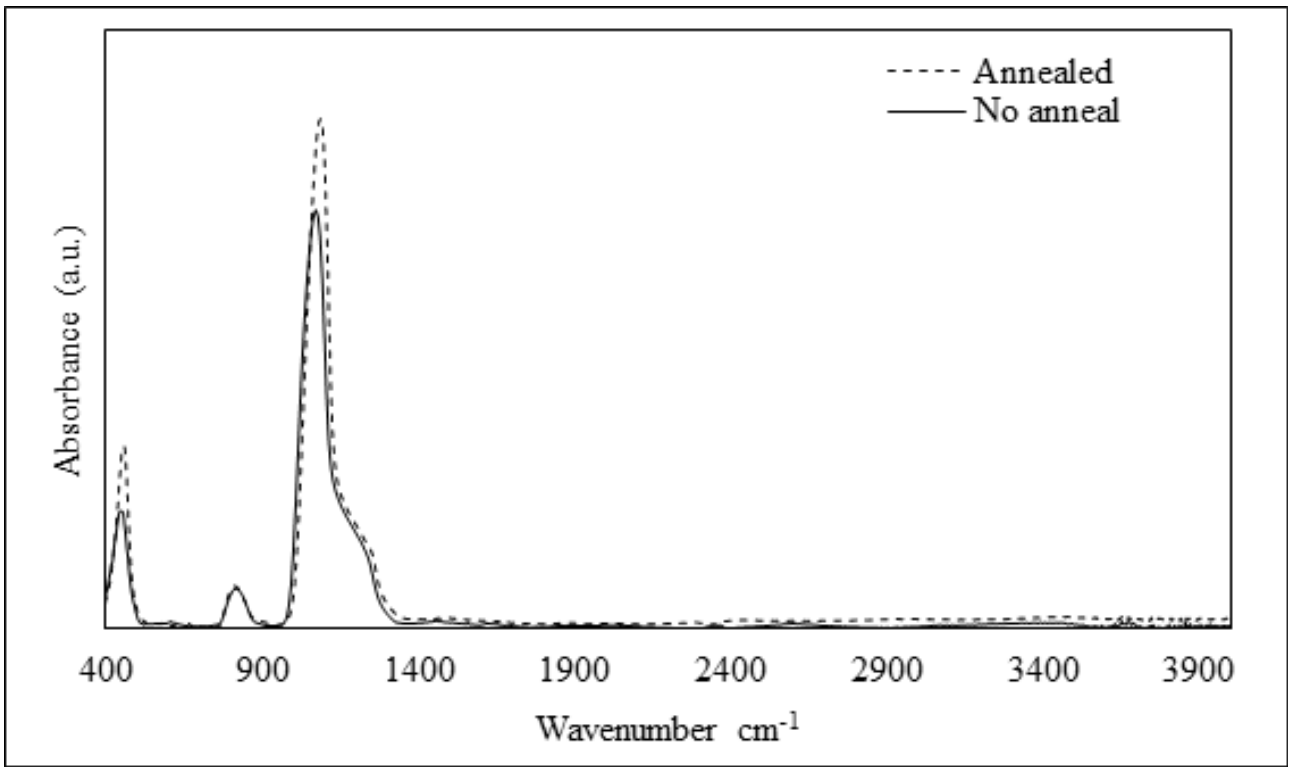


Figure 3: FTIR spectrum of SiO_2 film.

3.3. Residual stress

The stress within the silicon dioxide films is a critical parameter influencing their insulating performance. According to Table 5, the overall stress was found to increase with higher deposition pressure (Mahajan et al., 2004). Elevated pressure in the LPCVD furnace leads to a higher concentration of molecules and free radicals, increasing the likelihood that reactive species will impact the substrate surface with sufficient energy. This, in turn, promotes a higher deposition rate. At such elevated rates, the silicon content in the SiO_2 film tends to increase, which has been suggested to contribute to the higher stress levels observed (Ong et al., 2006).

However, the annealing process did not produce a significant change in the overall stress magnitude. Post-annealing stress is largely governed by annealing temperature and duration (Fu et al., 2017). In this study, annealing at 1000 °C for 60 minutes did not measurably alter the stress magnitude. Nonetheless, thermal treatment notably reduced the film curvature (1/μ), indicating partial relaxation or redistribution of stress gradients throughout the film thickness.

Table 5: Stress and curvature values of SiO_2 films.

Pressure (mT)	Sample	Stress (mPa)	Curvature (μ)	Curvature (1/ μ)
200	Non-annealed	-72.6±0.8	2.14±0.1	0.4672
	Annealed	-66.8±0.8	3.78±0.1	0.2645
300	Non-annealed	-118±1.2	3.36±0.2	0.2976
	Annealed	-129±1.0	4.59±0.6	0.2178
600	Non-annealed	-163±1.0	4.69±0.8	0.2132
	Annealed	-154±1.4	5.50±0.6	0.1818

3.4. Film density

In the study by Sometani et al., it was reported that the SiO_2 film thickness decreased after annealing, which was attributed to an increase in film density (Sometani et al., 2012). Their

investigation showed that SiO_2 film densities grown at deposition pressures of 200, 300, and 600 mT increased following annealing at 1000 °C for 60 minutes. Interestingly, as indicated in Table 6, the deposition pressure had no significant effect on the film density.

Table 6: Film densities of SiO2 films.

Pressure (mT)	Sample	Film Density (g/cm^3)
200	Non-annealed	2.171±0.03
	Annealed	2.240±0.03
300	Non-annealed	2.164±0.02
	Annealed	2.270±0.02
600	Non-annealed	2.184±0.02
	Annealed	2.260±0.02

3.5. Refractive Index

Pliskin, in his study, reported that the refractive index of SiO_2 films obtained via CVD processes increases with increasing film density (Pliskin, 1977). Similarly, McCann et al. investigated changes in the refractive index of LPCVD SiO_2 films annealed at various temperatures. They observed that the refractive index increased after annealing at temperatures ranging from 850 to 1000 °C (McCann et al., 2001).

According to the data presented in Tables 6 and 7, the annealing process resulted in an increase in the refractive index, which can be attributed to the concurrent rise in film density.

Table 7: Refractive index values of SiO_2 films.

Pressure (mT)	Sample	Refractive Index (632 nm)
200	Non-annealed	1.4573±0.001
	Annealed	1.4600±0.001
300	Non-annealed	1.4492±0.001
	Annealed	1.4567±0.001
600	Non-annealed	1.4484±0.001
	Annealed	1.4677±0.001

Table 7 also shows that the refractive index decreases with increasing deposition pressure. This decrease can be attributed to the higher desorption of TEOS-derived by-products on the SiO_2 film surface at elevated pressures. When the deposition pressure is high, a larger amount of TEOS is introduced into the system, resulting in an increased concentration of TEOS-derived by-products (Sometani et al., 2012).

3.6. Determination of contamination

Figure 4 presents AFM images of the silicon wafer surface following the removal of the silicon oxide layer. Figure 4-A shows a surface free of visible particles, indicating successful particle removal by the BOE solution treatment. However, Figure 4-B reveals the presence of small particles that were not eliminated by the BOE treatment. These particles are identified as unreacted radicals remaining on the silicon surface (Viana et al., 2001). It is suggested that these radicals may result from turbulence caused by the TEOS injector during the deposition process. The AFM image in Figure 4-B illustrates the silicon surface without TEOS radicals.

Furthermore, Raman analysis (Figure 5) supports these observations. The silicon oxide thin films exhibit punctual and large defects, as seen in Figure 4-B. These defects, referred to as "wafer defects," are associated with pre-existing line defects on the wafer surface. It is anticipated that the punctual defects share the same origin as the wafer defects. The Raman spectrum inside a punctual defect, shown in Figure 5, displays four distinct peaks at 1273, 1690, 2291, and 2809 cm^{-1} (Viana et al., 2001). The peak at 1273 cm^{-1} corresponds to aliphatic O–H bonds resulting from TEOS hydrolysis (Agarwal et al., 2011; Fischer et al., 2008)). The peak at 1690 cm^{-1} indicates the presence of C=C bonds. The peak at 2291 cm^{-1} is attributed to Si–H bonds (Gynba et al., 2003), while the peak at 2809 cm^{-1} represents C-H2 asymmetric stretching (Lam et al., 2011). The presence of C=C bonds confirms that unreacted radicals become trapped by surface structural defects (Viana et al., 2001). These bonds in the Raman spectrum indicate retention of by-products

formed during the gas-phase decomposition of TEOS within the film.

The primary intermediate species generated from TEOS under high-temperature gas-phase conditions include $Si(OH)(OC_2H_5)_3$ (triethoxysilanol), $O(Si(OC_2H_5)_3)$, C_2H_4, C_2H_5OH, and H_2O (Schoof et al., 2002). Among these, triethoxysilanol exhibits significantly higher surface reactivity compared to TEOS. Both TEOS and $Si(OH)(OC_2H_2)_3$ participate in surface reactions, depending on the surface coverage of ethoxy groups (Coltrin et al., 2000). However, due to the non-ideal reaction mechanisms occurring in the LPCVD furnace, undesirable by-products have been detected in the resulting oxide film.

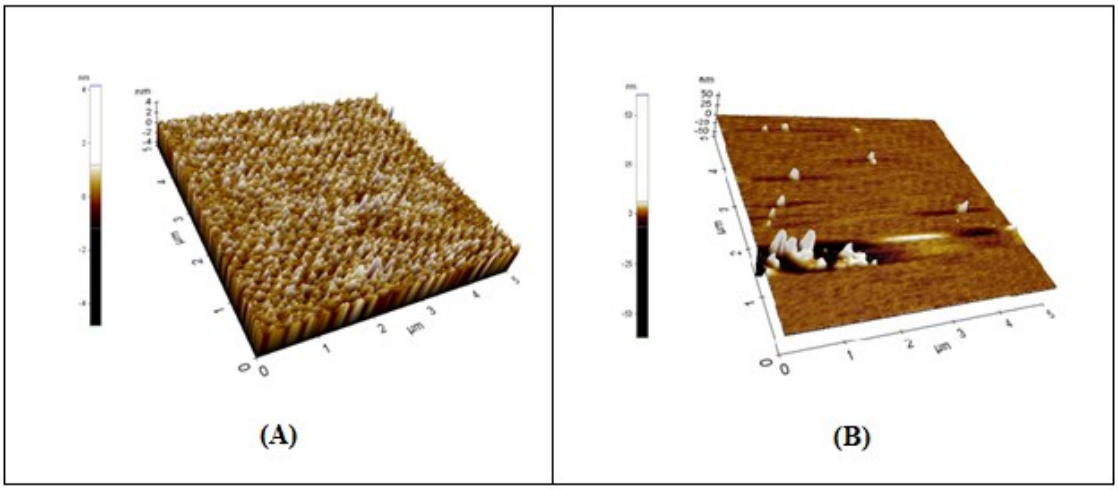


Figure 4: AFM images of the silicon wafer surface after removing the SiO_2 layer using a diluted BOE solution (A) Clean surface with no visible particles, indicating effective removal of residues **(B)** Surface with remaining fine particles, identified as unreacted radicals that were not removed by the BOE treatment.

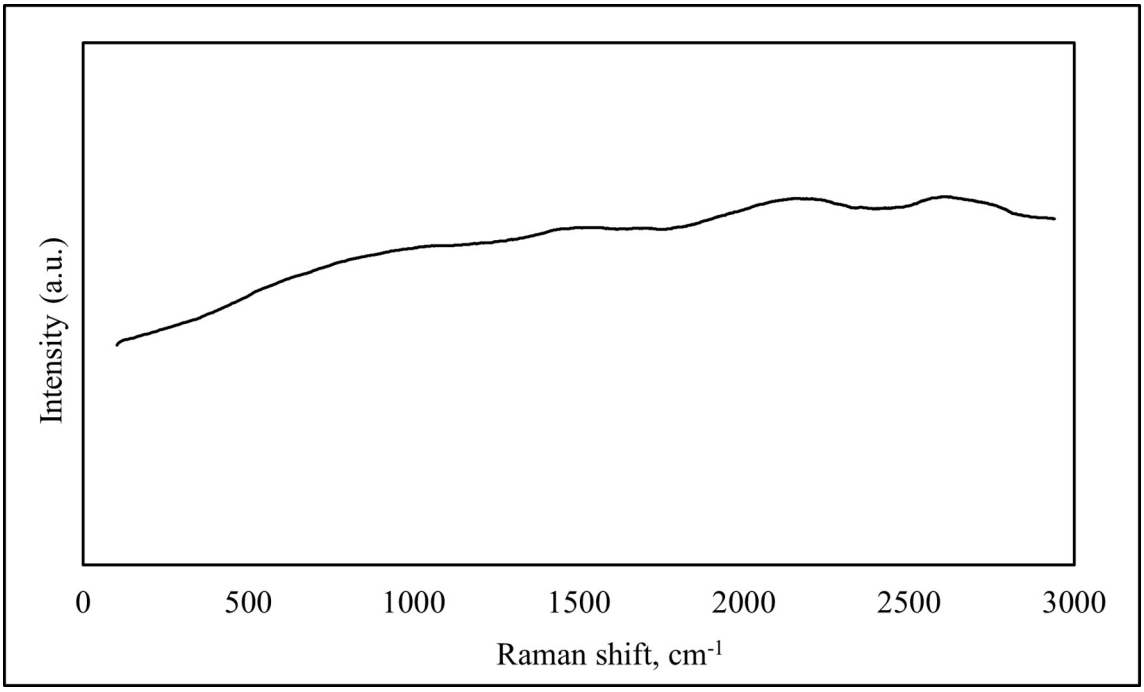


Figure 5: Raman spectrum of surface residues remaining after SiO_2 etching.

4. CONCLUSION

SiO_2 films were deposited using TEOS and O_2 gases in an LPCVD furnace at pressures ranging from 200 to 600 mT. Various characterizations were performed at different pressures to investigate the impact of annealing on the film structure. Additionally, a contamination analysis was conducted to assess the presence of specific bonds within the SiO_2 film.

The results showed that the SiO_2 growth rate increased with increasing pressure. However, no significant pressure-dependent changes in growth rates were observed, except for a decrease following annealing. The annealing process also induced shifts in FTIR peak positions, indicating structural modifications in the SiO_2 films.

Furthermore, both the deposition pressure and annealing influenced the film's stress, curvature, and refractive index. These properties were found to be affected by the deposition conditions and subsequent thermal treatment.

Contamination analysis detected specific bonds, including aliphatic O–H, Si–H, C–H2 asymmetric stretching, and C=C bonds. These are believed to originate from the pyrolysis of TEOS and its reaction with O_2 during deposition, indicating the presence of contaminants within the SiO_2 films.

Overall, this study provides insights into the growth of SiO_2 films, the effects of deposition pressure and annealing on film properties, and the identification of contamination-related bonds in the film structure.

5. REFERENCES

Agarwal UP, McSweeny JD, Ralph SA. FT–Raman investigation of milled-wood lignins: softwood, hardwood, and chemically modified black spruce lignins. Journal of Wood Chemistry and Technology 2011; 31: 324-344.

Bange JP, Patil LS, Gautam DK. Growth and characterızatıon of SiO2 films deposited by flame hydrolysis deposition system for photonic device application. Progress In Electromagnetics Research M 2008; 3:165-175.

Coltrin ME, Ho P, Moffat HK, Buss RJ. Chemical kinetics in chemical vapor deposition: growth of silicon dioxide from tetraethoxysilane (TEOS). Thin Solid Films. 2000; 365:251-263.

Fischer D, Pospiech D, Scheler U, Navarro R, Messori M, Fabbr P. Monitoring of the sol-gel synthesis of organic-inorganic hybrids by FTIR transmission, FTIR/ATR, NIR and raman spectroscopy. Macromolecular Symposia 2008; 265(1): 134-143.

Fu J, Shang H, Li Z, Wang W, Chen D. Thermal annealing effects on the stress stability in silicon dioxide films grown by plasma enhanced chemical vapor deposition. Microsyst Technol. 2017; 23:2753-2757.

Gerelt-Od M, Kolesnikova TG, Mokrushev PA, Vishnevskiy AS, Vorotilov KA, Gismatulin AA, Gritsenko VA, Baklanov MR. Exploring the relationship between electrical characteristics and changes in chemical composition and structure of OSG low-k films under thermal annealing. Coatings 2024; 14:1412.

Gnyba M, Jędrzejewska-Szczerska M, Keränen M, Suhonen J. Sol-gel materials investigation by means of raman spectroscopy. Proceedings XVII IMEKO World Congress 2003 June 22-27.

Holzer S, Sheikholeslami A, Karner M, Grasser T, Selberherr S. Comparison of deposition models for a TEOS LPCVD process. Microelectronics Reliability 2007; 47: 623-625.

Lam JCK, Huang MYM, Tan H, Mo Z, Mai Z, Wong CP, Sun H, Shen Z. Vibrational spectroscopy of low-k/ultra-low-k dielectric materials on patterned wafers. Journal of Vacuum Science & Technology A Vacuum Surfaces and Films 2011; 29(5): 051513-051513-6.

Li S, Xu J, Wang L, Yang N, Ye X, Yuan X, Xiang H, Liu C, Li H. Effect of post-deposition annealing on atomic layer deposited SiO_2 film for silicon surface passivation.

Materials Science in Semiconductor Processing 2024; 106:104777.

Mahajan AM, Patil LS, Gautam DK. Influence of process parameters on the properties of TEOS–PECVD-grown SiO2 films. Surface and Coatings Technology 2004; 188(1):314-318.

McCann P, Somasundram K, Byrne S, Nevin A. Conformal deposition of LPCVD TEOS. Proc. SPIE 2001; 4557.

Ong PL, Wei J, Tay FEH, Iliescu C. A new fabrication method for low stress PECVD-SiNx layers. Journal of Physics: Conference Series 2006; 34:764-769.

Pliskin WA. Comparison of properties of dielectric films deposited by various methods. Journal of Vacuum Science and Technology 1977; 14: 1064-1081.

Rajib A, Horita S, Rahman A, Ismail AB Md. Study of the influence of temperature on the deposition of SiO2 films from reaction of silicone oil vapor and ozone gas. Rajshahi University Journal of Science & Engineering 2016; 44: 1-8.

Ritala H. Kiihamaki J. Puukilainen E. Correlation between film properties and anhydrousHF vapor etching behavior of silicon oxide deposited by CVD methods. Journal of The Electrochemical Society 2011; 158(6): D399-D402.

Schoof GJ, Kleijn C, Van den Akker H, Oosterlaken TGM, Terhorst HJCM, Huussen F. Simulation and validation of SiO_2 LPCVD from TEOS in a vertical 300 mm multi-wafer reactor. Journal de Physique IV (Proceedings). 2002; 12:Pr4-51.

Seshan K. Handbook of Thin-Film Deposition Processes and Techniques Principles, Methods, Equipment and Applications. Noyes Publications William Andrew Publishing. Second Edition. Norwich, New York, U.S.A. 2002.

Sharma N, Hooda M, Sharma, SK. Synthesis and characterization of LPCVD polysilicon and silicon nitride thin films for MEMS applications. Hindawi Publishing Corporation Journal of Materials 2014. Journal of Materials 2014; 5.

Sometani M, Hasunuma R, Ogino M, Kuribayashi H, Sugahara Y, Uedono A, Yamabe K. Variation of chemical vapor deposited SiO2 density due to generation and shrinkage of open space during thermal annealing. Japanese Journal of Applied Physics 2012; 51(2): 110.

Vamvakas VE, Davazoglou D, Vahlas C, Thermodynamic study, compositional and electrical characterızatıon of Lpcvd SiO2 fılms grown from Teos/N2O mixtures. Microelectron. Reliab 1998; 38(2): 265-269.

Viana CE. Silva ANRD. Morimoto NI. Analysis of SiO2 thin films deposited by PECVD using an oxygen-TEOS-argon mixture. Brazilian Journal of Physics 2001; 31(2): 299.

Zanotti L. Rojas S. Doghiefu E. Santarelli E. Process characterization for Lpcvd Teos-Ozone Based SiO2 Films. J. Phys. IV France 1993; 3: C3-337-C3-343.

Zhi X, Li X, Yuan S, Wang D, Wang K. Influence of thermal annealing on mechanical and optical property of SiO_2 film produced by ALD. Materials 2024; 17:470.

Zhu X, Chen X, Liu H, Kang R, Zhang B, and Dong Z. An empirical equation for prediction of silicon wafer deformation. Materials Research Express 2017; 4(6)